

# Data-driven In-orbit Current and Voltage Prediction using Bi-LSTM for LEO Satellite Lithium-ion Battery SOC Estimation

Seok-Teak Yun and Seung-Hyun Kong, *Senior Member, IEEE*

**Abstract**—Accurate estimation of the battery system state of charge (SOC) is essential to the satellite mission design and fault management. However, it is difficult for low Earth orbit (LEO) satellites to continuously monitor the battery SOC on the ground due to the non-contact duration. To estimate the battery SOC for the entire orbit, it is necessary to predict or monitor the battery data for all times. Therefore, existing studies use SOC estimation that relies on real-time onboard battery information or utilizes probability-based technique and power budget-based technique. The real-time onboard-based technique is unsuitable for mission design because the status information is not available to the ground during the non-contact duration. Probability-based and power budget-based techniques are not reliable during the non-contact duration. In this study, we propose the ground-based battery SOC estimation technique that predicts the current and voltage by using bidirectional long short-term memory (Bi-LSTM) network for the non-contact duration and estimates the SOC by unscented Kalman filter (UKF) for all operating conditions. The proposed technique is tested with in-orbit data of the KOMPSAT-3A satellite, and we demonstrate its superior performance than other conventional ground-based SOC estimation techniques.

**Index Terms**—Bi-LSTM, LEO satellite, battery current prediction, battery SOC

## I. INTRODUCTION

LITHIUM-ION battery is widely used in satellite systems because of its multiple advantages, including high reliability, high voltage, high power density, acceptable heat generation, lightweight, and track verification [1,2,3]. For safety and guaranteed performance in their operating range, satellite systems require fault protection management design, one of which is the state of charge (SOC) monitoring [4,5,6]. The SOC estimation of the battery system for satellites directly determines available missions and fault management design [7,8]. In particular, an accurate and reliable battery SOC estimation technique for predicting the battery SOC during satellite operation is critical because a low Earth orbit (LEO) satellite system cannot be continuously monitored from the ground due to the non-contact duration [9]. In addition, determining possible missions to maximize the performance of

Seok-Teak Yun is with Robotics Programs, Korea Advanced Institute of Science and Technology (KAIST), 335 Gwahak-ro, Yuseong-gu, Deajeon, 305-701, Republic of Korea; Division of KOMPSAT-7 program, Korea Aerospace Research Institute, Gwahangno, Yuseong, Daejeon 34133, Republic of Korea (e-mail: yungun@kaist.ac.kr).

Seung-Hyun Kong is with the CCS Graduate school of Green Transportation, KAIST, 335 Gwahak-ro, Yuseong-gu, Deajeon, 305-701, Republic of Korea. (e-mail: skong@kaist.ac.kr). (*Corresponding author: Seung-Hyun Kong.*)

an LEO satellite is possible only when the SOC of the satellite battery is estimated accurately and reliably for all times.

The SOC of a battery system has nonlinear characteristics that depend on the current, voltage, and temperature. Therefore, the current and voltage of a battery, temperature data are required to estimate the battery SOC accurately [8,9]. In the case of LEO satellites, estimating the battery SOC requires the prediction of charging and discharging current and voltage during the non-contact duration. Because the charging and discharging currents and voltages vary depending on several factors, such as the satellite service life, orbit, and posture, it is difficult to predict them mathematically. LEO satellite power-related fault management design involves preventing additional error propagation that may occur when the battery is discharged or charged beyond certain conditions. Therefore, in the case of LEO satellites, when it is impossible to estimate future values accurately for a number of above mentioned factors, the possible mission design guidelines are conservatively assumed to conform to the worst case. Such a conservative design may lead to the cancellation of a mission in orbit or entry into a safe mode even if the state of the satellite battery is within the normal operating range. Therefore, precise prediction of the battery current and voltage and the estimation of the battery SOC are critical to the successful operation of LEO satellite systems.

The SOC of a lithium-ion battery system has been difficult to predict; it is a nonlinear system that relies on the use environment and conditions [10,11]. For SOC estimation, most of the studies use a circuit-model-based nonlinear estimation or a data-based estimation [12,13,14]. In the circuit-model-based estimation, the SOC is estimated using filters such as extended Kalman filter (EKF) and unscented Kalman filter (UKF) after circuit modeling using experimental data [15,16,17]. The data-based estimation uses a supervised learning algorithm in which long-term training data is used to train a deep neural network (DNN) [18,19,20]. Recent studies show that battery systems exhibit nonlinearity, with varying chemical characteristics depending on the environment, conditions, and duration of use, proving it more appropriate to estimate SOC using data-based models or simultaneously using data-based models and filters such as the EKF and UKF [14,20,21].

Because the existing battery state estimation techniques rely on using voltage, current, and temperature measured in real-time, the SOC estimation logic must be implemented onboard in satellite applications. Such an onboard implementation logic requires consideration of the throughput of the satellite flight

software and an additional verification process. In general, for satellites that require precise attitude control, the increase in throughput due to an additional logic can be burdensome. Moreover, because the onboard estimation is not transmitted to the ground continuously in real-time due to the non-contact duration, the onboard estimation can not be used for the mission design on the ground.

LEO satellite mission design on the ground requires prediction of the current and voltage or energy of the battery. Most existing studies focus on applications where the current and voltage can be measured in real-time [15-21]. Therefore, current and voltage modeling to estimate the battery SOC has not been considered. However, in the case of LEO satellites, access to the current and voltage data is limited, due to which predicting the current and voltage on the ground is required.

Therefore, this paper proposes a ground-based battery SOC estimation technique using UKF with predicted data as input during the non-contact duration, where the predicted data (i.e., battery current and voltage) is generated by the bidirectional long short-term memory (Bi-LSTM) model. To verify the proposed technique, feature extraction, preprocessing, and Bi-LSTM network design are tested with KOMPSAT-3A in-orbit data. The battery current and voltage and the accuracy of the orbit are compared with respect to the plenty of the learning dataset. Moreover, the SOC estimated using the actual current and voltage data are compared to the SOC estimated using the predicted current and voltage by the Bi-LSTM model.

The main contribution of this study is as follows.

- The proposed technique estimates the battery SOC by using the battery current and voltage predicted by Bi-LSTM as an input to the UKF in the non-contact duration. In the contact duration, the proposed technique can also continuously estimate the SOC using the real-time current and voltage. Therefore, the proposed technique allows an accurate and continuous ground-based battery SOC prediction for both the contact and non-contact durations of LEO satellites, which has been impossible with the conventional battery state estimation on the ground.
- In addition, the proposed technique performs accurate SOC estimation by employing in-orbit battery aging model. We demonstrate the superior performance of the proposed technique to the existing technique using the KOMPSAT-3A in-orbit data.
- Applying the proposed technique to LEO satellites, it becomes possible to design the maximally beneficial mission on the ground and to suggest battery management and protection guidelines.

This paper is organized as follows. Section II of this paper describes the KOMPSAT-3A satellite and the Bi-LSTM network used in this study. Section III describes the proposed LEO satellite battery state estimation technique. Section IV explains the characteristics of the in-orbit housekeeping data for the KOMPSAT-3A satellite, explains the necessity of preprocessing, and describes the hyperparameter optimization method. Section V analyzes the learning results for estimating the charging and discharging currents and voltages of the KOMPSAT-3A satellite. In addition, the technique of SOC and state of health (SOH) estimation method used in this study

and the test results are described. Finally, Section VI draws the conclusion of this paper.

## II. BACKGROUND

The battery current and voltage profiles have nonlinear characteristics, with respect to time, that change depending on the temperature of the solar array, satellite attitude, orbit, temperatures of the satellite body and payload, and the aging effects of the unit. Since Bi-LSTM can model nonlinear characteristics with good accuracy, we employ the Bi-LSTM network to predict the current and voltage of an LEO satellite battery.

This section introduces the KOMPSAT-3A satellite and battery system considered in this paper and briefly summarizes the Bi-LSTM network.

### A. KOMPSAT-3A Satellite

The KOMPSAT-3A satellite is an observation satellite developed by the Korea Aerospace Research Institute and is equipped with an electronic, optical camera with a resolution of 55cm. The satellite was launched using the Dnepr-1 projectile on March 26, 2015, and is operating in a solar-synchronous orbit at an altitude of 528km. KOMPSAT-3A performs functions including geographic information system (GIS) and environmental, agricultural, and ocean monitoring. A battery package was installed to supply power during such a mission, with the VES100 battery 4P12S developed by SAFT, as shown in Fig. 1. This study uses satellite housekeeping data for about three years after launch for data-based DNN development, modeling, and verification. The feature selection, network development, and training data are described in Section 4.

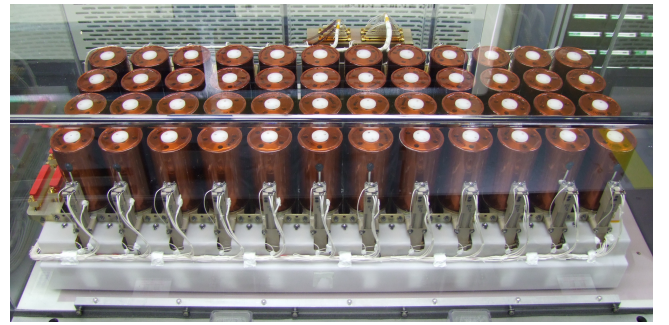


Fig. 1: KOMPSAT-3A battery package.

Each orbit period of the KOMPSAT-3A satellite can be divided into two duration, as shown in Fig. 2. First, there is a contact duration in which communication with the ground station is possible, and in-orbit data can be transmitted. Next, there is a non-contact duration in which there is no communication, and the satellite data is stored in the onboard memory. For most LEO satellites, the non-contact duration is considerably longer than the contact duration. Therefore, for the mission design of the satellite, the prediction of battery data corresponding to the non-contact duration is required. Since the existing research for estimating the satellite battery SOC is based on onboard, non-contact duration data is not

transmitted to the ground in real-time [12,13,16]. Therefore, it is not easy to use it for the ground-based mission design of the satellite. The power budget-based technique has been used for the possible mission determination. However, since the power budget-based prediction is calculated with assumptions, such as temperature and degradation, it is difficult to predict accurately and generalize to various satellites.

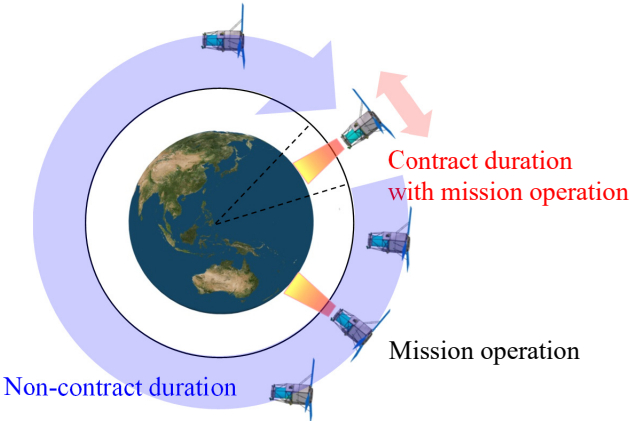


Fig. 2: KOMPSAT-3A contact and non-contact durations.

### B. Bi-LSTM Network

Long short-term memory (LSTM) is a network architecture robust to the vanishing gradient problem and addresses the long-term dependencies that arise with increasing sequence length in a recurrent neural network (RNN) [22]-[25].

Bi-LSTM is an extension of LSTM in which two LSTM models learn from the input data, one in the forward direction and the other in the backward direction. Bi-LSTM offers greater accuracy when there exists a meaningful pattern in the reverse direction [26,27]. Because satellite battery profiles exhibit significant patterns in both the forward and reverse directions, this paper proposes a battery current and voltage prediction model based on the Bi-LSTM network.

### III. PROPOSED BATTERY SOC ESTIMATION TECHNIQUE FOR LEO SATELLITE

We propose the data-based battery current and voltage prediction and UKF-based battery SOC estimation technique to maximize the satellite mission performance. Fig. 3 shows the flow of the DNN-based battery current and voltage prediction technique. First, features are selected to predict the battery current and voltage, and preprocessing is performed prior to learning. This preprocessing is to address the characteristics of the chosen features, outlier removal, interpolation, synchronization, normalization, and removal of data under specific situations for learning efficiency. Subsequently, a Bi-LSTM network is employed to model the current and voltage of the LEO satellite battery. A fully connected layer is added to both the input and output ends. Two Bi-LSTM layers are implemented because multiple Bi-LSTM layers are shown to improve accuracy [27]. Moreover, a dropout layer is placed after each of the two Bi-LSTM layers to prevent overfitting.

Next, optimization is performed to select hyperparameters (e.g., the number of Bi-LSTM hidden units, the initial learning rate, and the dropout rate) of the designed Bi-LSTM network. Since it is impossible to test all possible hyperparameters and datasets for optimization due to the computation cost, main hyperparameters and datasets are selected for optimization. We choose the root mean squared error (RMSE) to evaluate the objective function to train the network. We perform the evaluation using the learning and verification dataset until a predetermined number of iterations is reached or the objective function is converged. The hyperparameters, datasets, and objective functions are described in detail in Section IV.

The Bi-LSTM network is trained using the selected hyperparameters for performance analysis in the learning period. Fig. 4 shows the dataset used for training and performance analysis. For the KOMPSAT-3A satellite considered in this paper, we update the training dataset every month, assuming no rapid model changes, as shown in Fig. 4. We perform normalized output feature restoration based on the preprocessing procedures and compare the actual in-orbit values from the test dataset to analyze the prediction results.

Fig. 5 illustrates the proposed ground-based LEO satellite battery estimation technique in this paper. Using features such as the designed and predicted satellite attitude, orbit, and scheduled mission mode on the ground as inputs, the current and voltage of the satellite battery during the non-contact duration are predicted by the pre-trained Bi-LSTM network. The figure shows that the battery current prediction output is first obtained through the Bi-LSTM network. Then, the battery voltage prediction is performed by adding the predicted battery current as input to the Bi-LSTM network.

On the other hand, the actual battery current and voltage values are used after outlier removal in the contact duration. Moreover, the battery SOC is estimated using the UKF in all durations, including contact duration and non-contact duration, to ensure that the errors can not diverge. In this paper, considering the orbit of KOMPSAT-3A, we provide analysis under the assumption that the maximum non-contact duration is less than one-day. In addition, the battery capacity is monitored based on the satellite voltage profile during the mission and reflected in the state model for SOC estimation. The aging measurements of the battery are collected with a cycle of one month, as there are no rapid fluctuations.

### IV. PREPROCESSING AND HYPERPARAMETER SELECTION FOR BATTERY CURRENT AND VOLTAGE PREDICTION

For data-driven modeling using the in-orbit housekeeping data of the KOMPSSAT-3A satellite, it is necessary to understand the data generated by the satellite. In general, housekeeping data regarding the state of an LEO satellite is recorded with a specific period determined by the downlink and storage capacity. In addition, radiation from the space environment may cause temporary outliers in the satellite orbit data. Therefore, filtering outliers is necessary for data-driven modeling. Additionally, exceptional in-orbit data can be generated that may affect the correlation, depending on the target to be estimated. The exceptional in-orbit data can affect

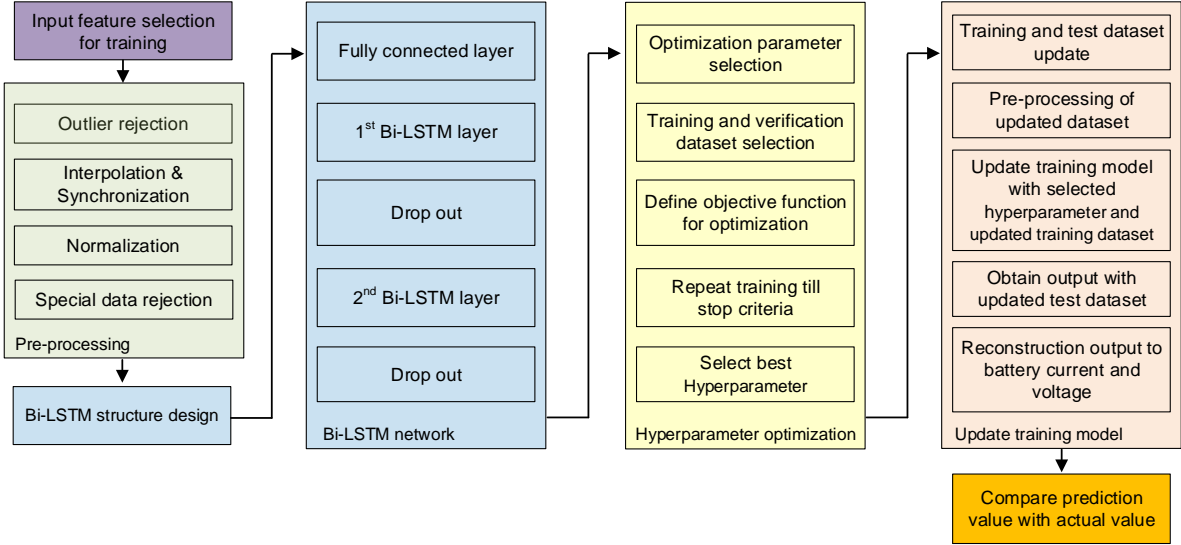


Fig. 3: Flow of the proposed Bi-LSTM-based battery current and voltage prediction technique.

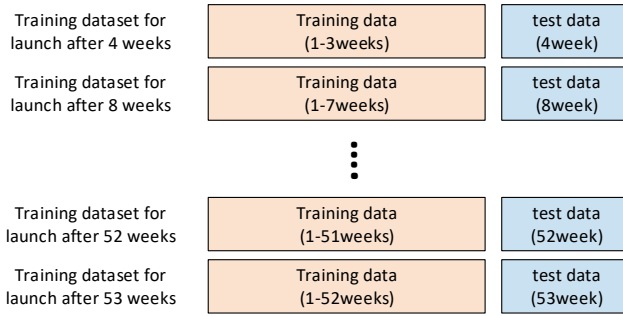


Fig. 4: Updated dataset over time after launch.

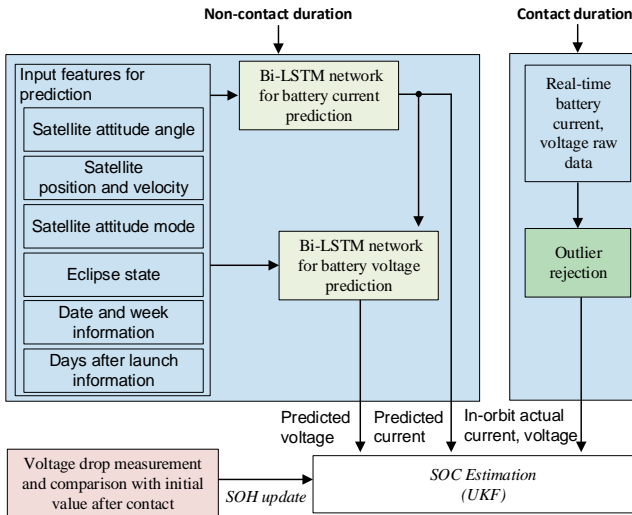


Fig. 5: Concept diagram of proposed ground-based LEO satellite battery SOC estimation technique.

the prediction accuracy. For example, when modeling the current profile in the normal state of the satellite, abnormal or exceptional case features that may impair the accuracy of the model should be excluded. Finally, because long-term time-series data must be used to estimate the changes in the model during the mission, it is also necessary to select appropriate features. In this section, the preprocessing procedure for model construction and hyperparameter selection are described.

#### A. Feature Selection

Table I shows the features used to estimate the current and voltage profiles of the LEO satellite battery. The features include the data that can be predicted or designed on the ground and values that can describe degradation and aging.

First, the position, orbital velocity, eclipse state, and quaternion of the attitude are selected as predictable features on the ground and highly correlated to the battery current and voltage. Because the attitude command of the satellite takes the form of quaternion data in the Earth-centered inertial (ECI) coordinate frame in KOMPSAT-3A, the attitude command should be converted into the maneuvering angle to reduce the dimensionality. The coordinate frame is changed to the local vertical local horizontal (LVLH) using the direction cosine matrix (DCM) as below for intuitive manipulation,

$$\text{DCM for ECI to LVLH} = \begin{bmatrix} (\frac{(v \times r) \times r}{|(v \times r)|^2})^T \\ (\frac{(v \times r)}{|(v \times r)|})^T \\ -(\frac{r}{|r|})^T \end{bmatrix}, \quad (1)$$

where  $r$  is the satellite position vector and  $v$  is the velocity vector in the ECI coordinate frame.

The eclipse state is divided into four types (e.g., Eclipse, Eclipse-to-sun transition, Sun, Sun-to-eclipse transition) and converted into integers from 1 to 4 respectively for modeling. We also add the operational mission mode and the attitude mode, which are features that can be designed on the

TABLE I: Input features for battery current and voltage prediction

	Feature	Unit
Features for battery current prediction	Satellite attitude in LVLH ( <i>roll, pitch, yaw</i> )	degree
	ECI position vector ( <i>x, y, z</i> )	km
	ECI velocity vector ( <i>x, y, z</i> )	km/s
	Satellite attitude mode	integer (1 to 4)
	Satellite mission mode	integer (1 to 5)
	Eclipse state	integer (1 to 4)
	Date information	integer (1 to 31)
	Week information	integer (1 to 52)
Features for battery voltage prediction	Same features as current prediction	
	Battery current	A

ground. Similar to the eclipse state, all categorical features are converted into integers. Accordingly, the attitude mode of the satellite (e.g., Normal, Sun pointing, Image, Nadir) is converted into values from 1 to 4, and the mission mode is converted into values from 1 to 5 to represent standby, ready, imaging, imaging and downlink, and off. In addition, the date, week, and days after launch are included as features to reflect seasonal characteristics and degradation effects.

Because the battery voltage varies with respect to the battery current, the battery current should be included as an input feature to the Bi-LSTM network for battery voltage prediction. That means, the battery current is first predicted and used as an input for battery voltage prediction. All input features are predictable or correspond to values determined through the mission design.

### B. Outlier Rejection

In general, satellites operate in a harsh radiation environment. Therefore, single event upsets (SEUs), single event transients (SETs), and instantaneous outliers occur in the housekeeping data due to the harsh environment. Outliers can compromise the accuracy of the learning model and must be removed. The distinctive properties of these outliers show significant changes from the previous state relative to other features or show physically impossible values.

The raw battery current and voltage data of KOMPSAT-3A are shown in Fig. 6. In this figure, a positive value of the battery current represents a charging current, and a negative value represents a discharging current. The figure shows an example of an outlier, the data point with a blue circle. In this study, outliers are removed based on the nominal threshold range of each feature.

### C. Data Interpolation and Normalization

LEO satellites deliver housekeeping data at several cycles within the downlink budget because of the limited access time to the ground station. Therefore, the period of the housekeeping data and the storage time are different. In addition, when an outlier is removed, a time point with no information occurs. As a result, synchronization through interpolating these data points is necessary to compensate for the removed points.

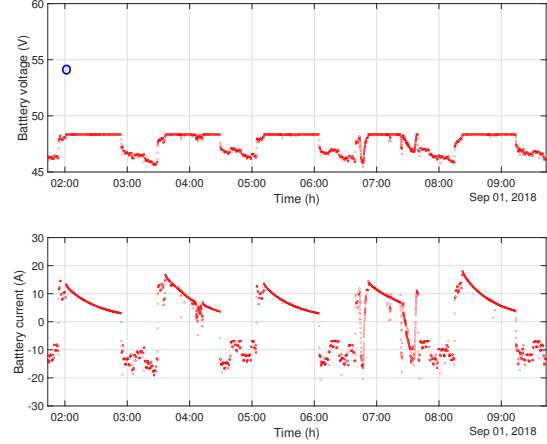


Fig. 6: An outlier in the battery voltage housekeeping data.

The satellite features used in this study are of several mixed data types. Data with various scales and ranges, such as orbit, attitude, current, and voltage, and categorical data, such as the mission mode, are included. For example, the battery voltage range is from 30 to 50V, and the satellite angle range is from 0 to 360 degrees. In addition, the orbital position is in kilometers, and the orbital velocity is kilometers per second. Therefore, using these data directly for learning could make optimization difficult near a local minimum or fail in model learning. Moreover, because the optimization performed for data-driven learning is based on gradient descent, data normalization is required to minimize the convergence time and prevent the optimization process from becoming trapped in a local minimum.

In general, the min-max and z-score are widely used for normalization [28]. Min-max normalization has the advantage of processing all features at the same scale but is sensitive to outliers. In this study, outliers are removed based on the nominal threshold range; therefore, as shown in (2), the min-max normalization is used to process all features at the same scale.

$$X_{\text{normalization}} = \frac{X - \min(X)}{\max(X) - \min(X)}, \quad (2)$$

where  $X_{\text{normalization}}$  represents a normalized feature,  $X$  represents the raw data of a feature,  $\min(X)$  denotes the minimum value of a feature, and  $\max(X)$  denotes the maximum value of a feature.

The KOMPSAT-3A housekeeping data after normalization and linear synchronization are shown in Fig. 7.

### D. Special Case Data Rejection

LEO satellites are generally designed to include a safe mode against potential system errors. In the safe mode, the system units used in the normal operation are limited to minimize power consumption to maintain a safe state of power and temperature. Fig. 8 shows the differences in the battery current and voltage profiles between the normal and safe modes of

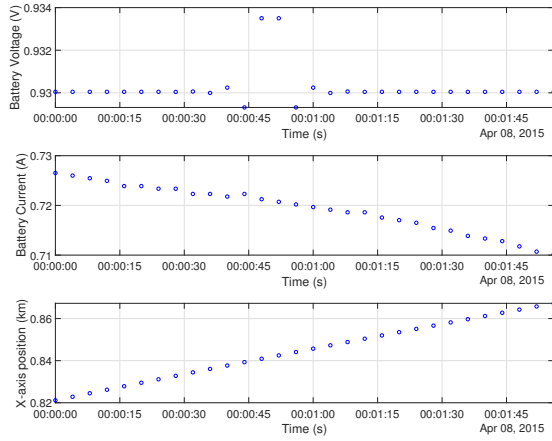


Fig. 7: Battery current, voltage, and X-axis position housekeeping data after normalization and synchronization.

KOMPSAT-3A. As shown, because the safe mode focuses on the stability of the satellite and limits the satellite resources, the amount of power produced and the power consumption are different from those in the normal mode. Since significant satellite errors usually occur at low frequency, the safe mode has a short period of operation for all satellite life. As a result, using safe mode data as training data may cause overfitting, which would impair the accuracy of the current and voltage prediction models for a normal operation. The purpose of this study is to estimate the state of the battery based on the prediction of the battery current and voltage profiles in the normal satellite operation.

Therefore, the housekeeping data during the satellite operation in the safe mode are removed from the data used for learning. For this purpose, the categorical satellite mode is used for rejection. After normalization, data with values of less than 0.2, corresponding to the safe mode, is not used for learning. A future study may investigate a method of predicting the state of the satellite outside the normal operation mode.

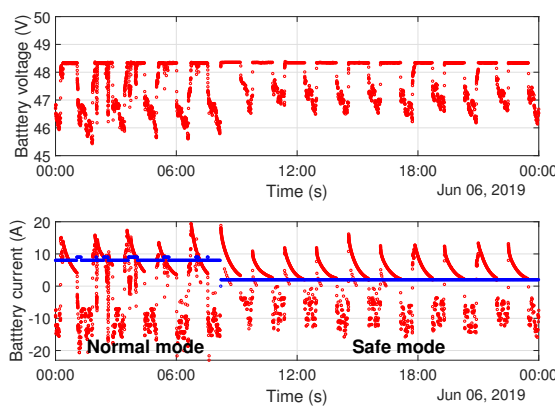


Fig. 8: Voltage and current profiles of normal mode and safe mode.

### E. Bayesian Hyperparameter Optimization

Data-based learning requires the selection of hyperparameters of the network. In this study, Bayesian optimization is used to optimize selected hyperparameters.

In practice, it is challenging to perform Bayesian optimization for all possible hyperparameters of a complex structure DNN [29,30]. It would take too much time to use all the data or to find the fully optimized configuration of all hyperparameters. The distinction between training data and verification data also dramatically affects the results. Therefore, assumptions are needed to select hyperparameters for Bayesian optimization. In this study, hyperparameters optimization is performed using data from one to six months after launch. Fig. 9 shows the training and verification datasets for hyperparameter selection. The selected main hyperparameters include the number of Bi-LSTM hidden units, the initial learning rate, and the dropout rate. Since the mean error is important for the power analysis of the satellite, the RMSE is chosen as the cost function

$$\text{Cost function} = \sqrt{\frac{1}{n} \cdot \sum (x - x^*)^2}, \quad (3)$$

where  $x$  is the actual value and  $x^*$  is the predicted value.

Moreover, the expected improvement and the Matérn 5/2 kernel, which are known to deliver good performance in general, are used as the acquisition function and the kernel function, respectively [30]. In the case of the KOMPSAT-3A satellite, when the objective function is calculated using data from one month to six months after launch, there is no significant difference observed in the optimal hyperparameters by dataset duration. Therefore, the hyperparameters are selected using the six months dataset. Meanwhile, the battery current and voltage predictions show relatively little influence by the dropout factor; however, it is confirmed that the effects of the depth of the Bi-LSTM layer and the initial learning rate are significant. As a result, the hyperparameters selected in this study are summarized in Table II.

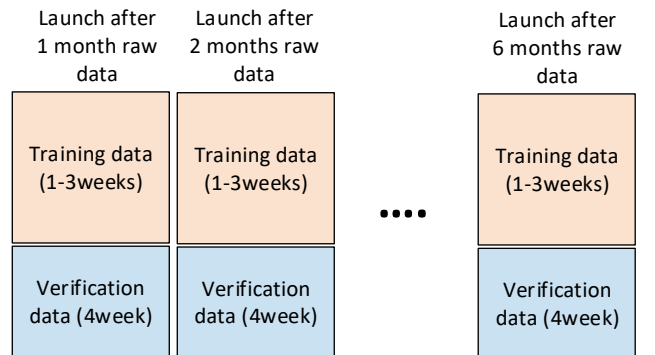


Fig. 9: Dataset for hyperparameter selection.

## V. IN-ORBIT PREDICTION RESULT

This section analyzes the estimation results of the actual (i.e., in-orbit) battery current and voltage based on the preprocessing procedure described in Section IV and the learning

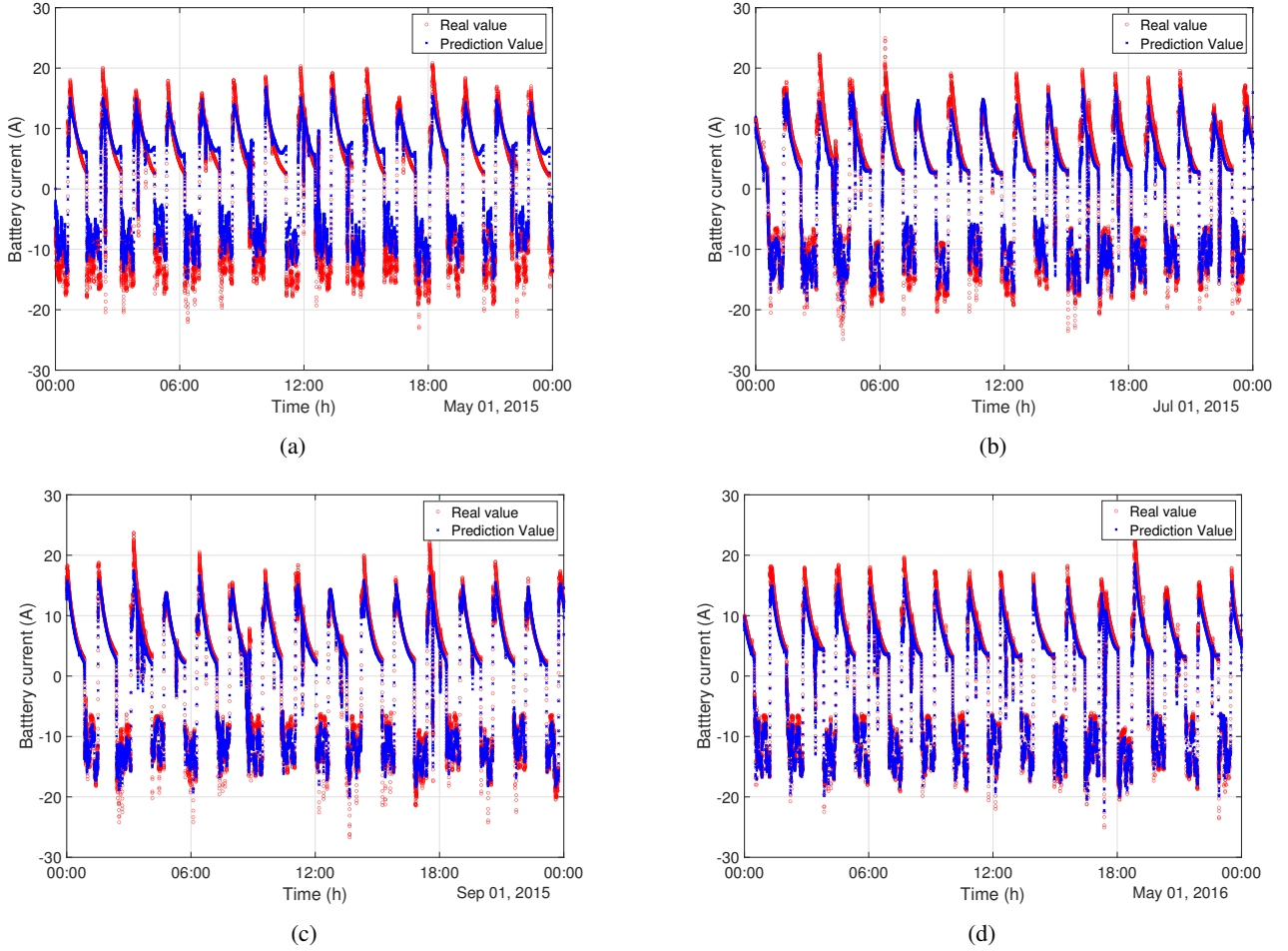


Fig. 10: Battery current prediction result: (a) Result for May.1st.2015; (b) Result for July.1st.2015; (c) Result for September.1st.2015; (d) Result for May.1st.2016.

TABLE II: Hyperparameters for deep Bi-LSTM network

Parameter	Current	Voltage
Optimizer	ADAM	ADAM
Initial learning rate	0.0994	0.0814
Number of 1st and 2nd Bi-LSTM hidden unit	40	30
Minibatch size	128	128
1st and 2nd dropout factor	0.3	0.3

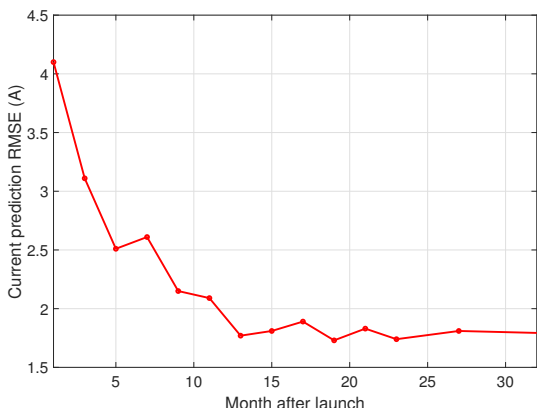


Fig. 11: Battery current RMSE after launch.

results obtained through the trained network. In addition, the SOC prediction results obtained using the predicted battery current and voltage are compared to various SOC estimation results; the SOC obtained using the actual housekeeping data of the satellite, the SOC based on power prediction using the seasonal autoregressive integrated moving average (SARIMA), and conventional power budget SOC analysis.

#### A. In-orbit Battery Current and Voltage Prediction Results

The battery current and voltage prediction comparison analysis presented in this paper is performed using data from the first day of each month. Fig. 10(a),(b),(c), and (d) show a one-day comparison of the Bi-LSTM-based current prediction model trained with about 4, 13, 21, and 53 weeks of the dataset. The blue dots represent the battery current predicted by the trained Bi-LSTM network, and the red circles represent the actual battery current data collected in orbit. A positive value of the battery current corresponds to a charging current, and a negative value corresponds to a discharging current. The maximum error is 9.88A, and the RMSE is 4.10A in Fig. 10(a). The maximum error of the current estimation for the data from 13 weeks after launch is 10.8A, and the RMSE is 3.11A, as in

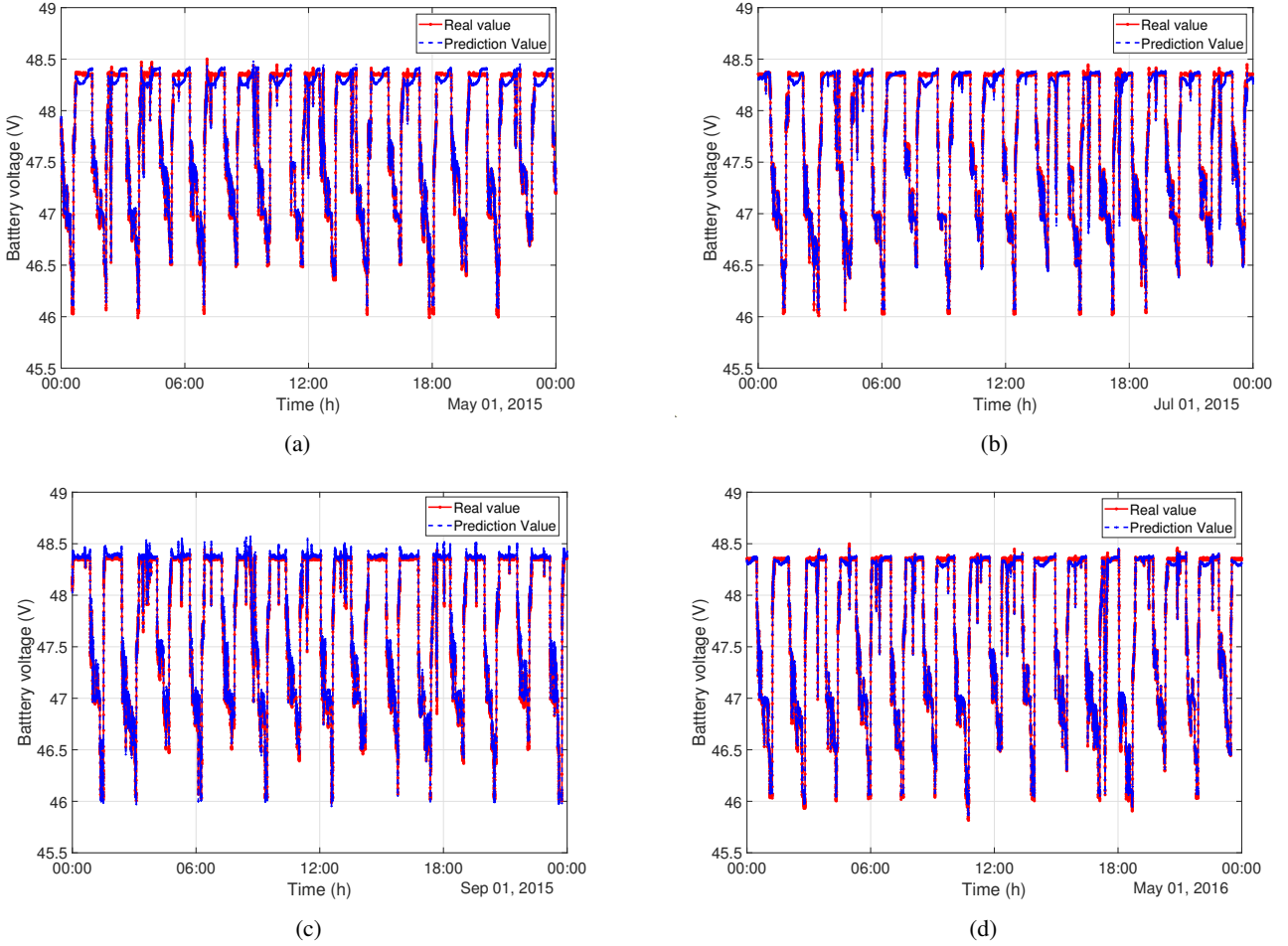


Fig. 12: Battery voltage prediction result: (a) Result for May.1st.2015; (b) Result for July.1st.2015; (c) Result for September.1st.2015; (d) Result for May.1st.2016.

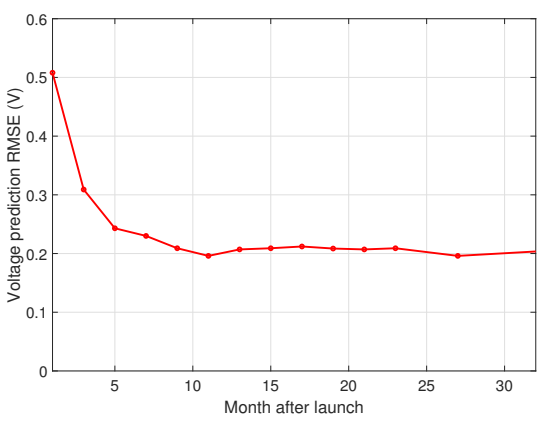


Fig. 13: Battery voltage RMSE after launch.

Fig. 10(b). At 21 weeks, the maximum error is 6.92A, and the RMSE is 2.51A, as in Fig. 10(c). At 53 weeks, the maximum error is 3.91A, and the RMSE is 1.77A, as in Fig. 10(d). It is confirmed that the performance in terms of both the maximum error and the RMSE is improved with an increasing length of the training period.

Fig. 11 shows the battery current RMSE calculated with the actual satellite data and the predicted data based on one-week data collected at two-month intervals. As seen in this figure, the performance stabilizes with the updating of the training data. This figure illustrates that battery current estimation is possible under various operating and environmental conditions.

Regarding the battery voltage, some difference from the actual value is inevitable due to the model error and the error of the predicted current value used as input. Fig. 12(a),(b),(c), and (d) show a one-day comparison of the predicted and actual values for about 4, 13, 21, and 53 weeks of training data, respectively. The blue dots represent the value predicted by the trained Bi-LSTM network, and the red circles represent the value collected on the actual orbit. The RMSE value is 0.51V for the case of 4 weeks training data. As shown in Fig. 12(a), the estimated overall performance is similar, but the predicted current discharge timing is earlier than the actual time, so an error occurs in the voltage in the taper charging section. Fig. 12(b) shows a comparison of the actual and estimated values at about 13 weeks after launch, where the RMSE value is 0.31V. Fig. 12(c) and 12(d) show the voltage predictions for 21 weeks and 53 weeks after launch, respectively. The voltage

RMSE after 21 weeks is 0.21V. After 53 weeks, the RMSE between the predicted and actual voltage values is 0.20V. It is demonstrated that the accuracy of the model increases with the amount of training data.

Fig. 13 shows the voltage RMSE for a one-week duration with respect to the amount of data used for training. Similar to the current in Fig. 11, the performance is improved as the data used for training is updated and accumulated.

### B. Battery SOC Prediction Technique

Battery SOC estimation can be performed by Ah-counting using current measurement, Kalman filter-based estimation using circuit modeling, and DNN. [20,31,32].

The Ah-counting has low computational complexity, but it is not suitable for continuous SOC estimation because errors are accumulated. Therefore, we compare the estimation results based on EKF, UKF, and DNN, using the ground test results before launch. To estimate the battery charging state using EKF and UKF, the state equation based on the circuit model in Fig. 14 is applied [33,34]. In general, the SOC can be calculated as [33]

$$SOC = SOC_o - \frac{1}{Q} \cdot \int I_T dt, \quad (4)$$

where  $Q$  is the battery capacity,  $SOC_o$  is the initial SOC, and  $I_T$  is battery current.

In the case of the satellites battery systems, a cell balancing circuit for reliability and uniformity between cells is included, or screening is performed. Therefore, in the case of  $m$  series and  $n$  parallel structures, a battery circuit model can be simplified as [35]

$$v_d = -\frac{m \cdot v_d}{n \cdot R_d \cdot C_d} + \frac{I_T}{C_d} \quad (5)$$

where  $v_d$  is polarization voltage, and  $R_d$  and  $C_d$  are represent characteristics for current, and

$$h(OCV, V_d) = V_T = OCV - V_d - R_I \cdot I_t, \quad (6)$$

where  $OCV$  is the open circuit voltage,  $V_T$  is battery terminal voltage,  $R_I$  is a series resistance representing an instantaneous voltage characteristic.

The KOMPSAT-3A satellite battery system has 12 series and 4 parallel cell structures with a balancing circuit. Consequently, simplified equations in (5) and (6) are used for the battery circuit model of the KOMPSAT-3A satellite.

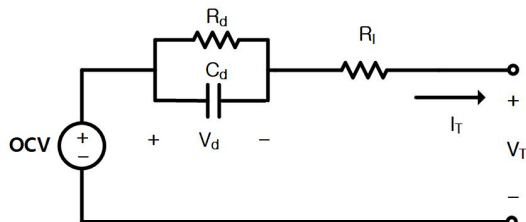


Fig. 14: Battery circuit model.

And the discrete-time state transition function using (4) and (5) can be found as

$$f(SOC, v_d) = \begin{bmatrix} SOC_{(k+1)} \\ v_{d(k+1)} \end{bmatrix} = \begin{bmatrix} 1 & 0 \\ 0 & e^{\frac{-T_s}{R_d \cdot C_d}} \end{bmatrix} \begin{bmatrix} SOC_{(k)} \\ v_{d(k)} \end{bmatrix} + \begin{bmatrix} \frac{-T_s}{Q} \\ R_d \cdot \frac{m}{n} \cdot (1 - e^{\frac{-T_s}{R_d \cdot C_d}}) \end{bmatrix} \cdot I_T, \quad (7)$$

where  $T_s$  is the sampling time.

On the other hand, open-circuit voltage (OCV) can be expressed as a function of the SOC and temperature. However, in the case of satellite batteries, temperature control is essential, and the range of temperature change is relatively small. Fig. 15 shows the temperature range of the satellite battery considered in this study. As shown, the range of temperature change is not wide, which does not affect the OCV calculation significantly. Therefore, the OCV is modeled as a function of the 6th order polynomial of SOC using the curve fitting as

$$OCV = P_6 \cdot SOC^6 + P_5 \cdot SOC^5 + \cdots + P_0, \quad (8)$$

where  $P_0, P_1, \dots, P_6$  represent the polynomial coefficients.

Using (6)-(8), the state-space and measurement model equations become

$$x_{k+1} = f(x_k, u_k) + w_k \quad (9)$$

$$y_k = h(x_k, u_k) + v_k, \quad (10)$$

where  $x_k$  is the state variable which includes  $SOC$  and  $V_d$ , and  $u_k$  and  $y_k$  represent the system input and ouput respectively.  $w_k$  is the Gaussian process noise with covariance  $Q_k$ , and  $v_k$  is the measurement noise with covariance  $R_k$ .

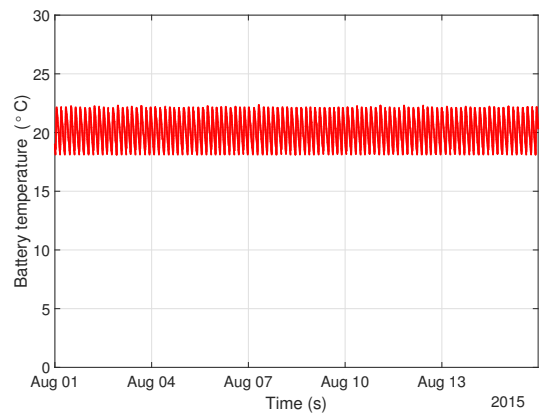


Fig. 15: Battery temperature during 16 days.

Table III describes the network hyperparameters used for the DNN-based SOC estimation, where the current and voltage of the battery are used as input. For DNN design, the number of hidden neurons, number of hidden layers, initial learning rate, and activation function are selected, as shown in Table III.

Fig. 16 shows EKF, UKF, and DNN-based estimations on the ground. Reference SOC is measured by calibrated

TABLE III: Hyperparameters for DNN network-based SOC estimator

Parameter	Value
Initial learning rate	0.0891
Number of hidden neurons	50
Number of hidden layers	6
Activation function	Sigmoid

Ah-counting based on current measurement, and the same sampling time is used for EKF, UKF, and DNN. The ground test is performed for fifteen orbits and the power consumption of the bus and payload according to the mission mode in both the eclipse and sun duration. In addition, Table IV shows the RMSE and maximum error of the estimation results of EKF, UKF, and DNN. As shown in Fig. 16 and Table IV, it is confirmed that the UKF-based SOC estimation error is the smallest and most reliable.

The SOC using DNN requires sufficient training, verification, and testing data. In particular, for SOC estimation, accurate measurement for reference is necessary. However, it is difficult to collect sufficient data for data-based SOC estimation in space applications. We do not run various ground tests for the satellite battery-package system due to the limited ground operating conditions, risks, and the additional cost of flight models. In the case of KOMPSAT-3A, only ground test data for fifteen orbit missions, three short missions, and two constant charge and discharge (C/10, C/5) data are available as a reference for training. As a result, as shown in Table IV, the estimation performance using DNN is not excellent. In addition, it is not easy to obtain accurate reference training data for the aging of battery-package systems in orbit.

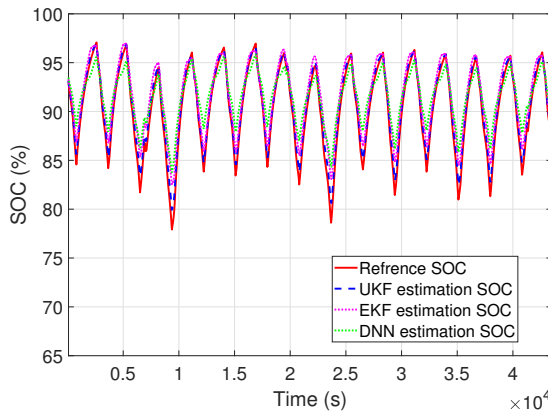


Fig. 16: SOC estimation result on ground test.

TABLE IV: SOC estimation error in ground tests

	EKF	UKF	DNN
RMSE	3.25 %	1.35 %	3.33 %
Maximum error	4.71 %	1.95 %	4.89 %

As a result, we propose UKF-based SOC estimation for both the non-contact and contact durations, which can reflect aging by modeling parameters and has a relatively small error. For the non-contact duration, the UKF utilizes the predicted value

by the trained Bi-LSTM network, and for the contact duration, the UKF uses the actual downlink value as an input.

To reflect the degradation of the satellite battery on the SOC estimation, capacity change is estimated using satellite in-orbit data. In general, to measure the SOH of a battery, there is a voltage measurement technique utilizing a specific square discharge current [36]. In the case of KOMPSAT-3A, a similar short-duration discharge current is generated when performing a mission. Therefore, even if no current is artificially applied, the battery SOH can be estimated through voltage measurement during the mission. The frequency-domain of battery terminal voltage is derived for the circuit model in Fig. 14 as [35]

$$V_T(s) = OCV(s) - I_T(s) \cdot \left( \frac{R_d}{1 + R_d \cdot C_d \cdot s} + R_I \right). \quad (11)$$

Using (11), (12) can be obtained assuming that the OCV of the short duration is constant as

$$\frac{\Delta V_{mission}}{\Delta I_{mission}} = \frac{m \cdot R_d}{n \cdot (1 + (m/n)^2 \cdot R_d \cdot C_d \cdot s)} + R_I. \quad (12)$$

Since the amount of change and the time interval of current and voltage are known,  $R_d$  and  $R_I$  can be calculated using (12). Since  $R_I$  increases as the battery system ages,  $R_I$  variation is considered to estimate the available capacity [37]. Fig. 17 shows the change in capacity according to the mission of the satellite considered in this study. Using the results of Fig. 17, the amount of capacity change during the operating period is reflected in the UKF model parameters.

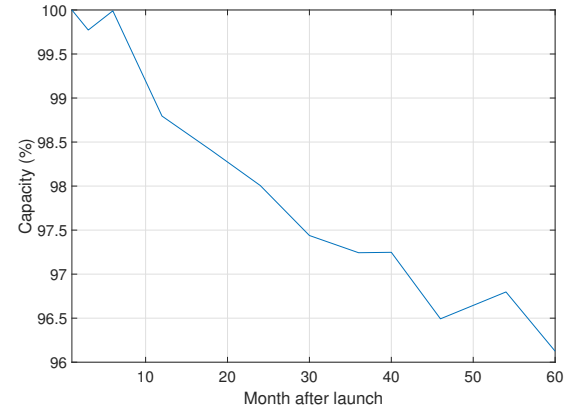


Fig. 17: Capacity variation during operation duration.

### C. In-orbit Battery SOC Prediction Results

To analyze the performance of the proposed SOC estimation technique for all durations, including the non-contact duration, we compare to the conventional techniques based on the power budget-based model and probability-based SARIMA model that uses satellite power demand and generated power.

The power budget-based model is generally used in the design stage to simplify the power generation and power consumption predictions. The battery SOC is defined in terms of

the difference between the generated power and the consumed power by the satellite. The generated power is defined as

$$P_G = P_{CA} \cdot D_{SA} \cdot C_{TEM} \cdot \cos(\theta_{SA}), \quad (13)$$

where  $P_G$  is the generated power,  $P_{CA}$  represents the solar array capacity,  $D_{SA}$  is the degradation factor of solar array,  $C_{TEM}$  is the solar array temperature coefficient, and  $\theta_{SA}$  is the angle of solar array perpendicular to the sun. And, the power consumption of the satellite is defined as

$$P_C = \sum(P_{unit}(mode) \cdot E_c), \quad (14)$$

where  $P_C$  is the total consuming power,  $P_{unit}(mode)$  represents the consuming power of each unit in the operation mode, and  $E_c$  is the power efficiency of each unit.

As shown in (13) and (14), the power analysis from the power budget perspective includes uncertainty factors such as degradation, solar array temperature, angle, and load efficiency. Therefore, the actual orbit power difference can be expressed using the uncertainty factors. As a result, the analysis through the power budget in this paper is modeled based on the maximum power consumption by the satellite unit.

To predict the battery charge state using generation and consumption powers, we use probability-based analysis, such as the autoregressive integrated moving average (ARIMA) model that predicts time-series data [38]. The ARIMA model has the advantage of deriving a useful model only with past observations and error terms but has the disadvantage due to unclear expression for the seasonality of the data. Seasonal autoregressive integrated moving average (SARIMA) adds a seasonality factor to ARIMA [39]. In the case of the KOMPSAT-3A satellite, the generation and consumption powers have seasonal characteristics, so the power prediction using SARIMA is performed and compared with the proposed technique. The training dataset for the SARIMA model is from the same duration used for the Bi-LSTM model, as shown in Fig. 4. In this paper, power generation and consuming SARIMA model parameters are  $(2,1,2)(2,1,4)4$ , which minimizes Bayesian information criterion (BIC).

Using the generated power and consumed power predicted by the power budget and SARIMA models, the charging and discharging power of the battery can be modeled, and the battery SOC can be defined as

$$SOC = \frac{E_R}{E_C} \cdot 100, \quad (15)$$

where  $E_R$  is the remaining battery energy, and  $E_C$  is the capacity of battery energy.

It is impossible to measure the actual SOC of a battery in orbit. However, as in Table IV, the estimated SOC using the UKF shows a slight error from the actual SOC through the ground test. In general, real-time download of satellite data is possible only during the contact duration. The satellite data in the non-contact duration is stored and transferred to the ground in the contact duration by playback. Consequently, we can use the past non-contact duration data after contact. Therefore, in this paper, the result of using the actual measured current

and voltage values, over all duration including non-contact duration, as input to the UKF is used as the in-orbit reference SOC.

A sufficient mission optimal design is possible for the KOMPSAT-3A satellite with data of one-day prediction considering the ground contact duration. Therefore, one day is set as the standard duration for SOC analysis. A comparison of the one-day battery SOC estimation using the satellite in-orbit data and the predicted data is shown in Fig. 18. Figs. 18(a), 18(b), 18(c), and 18(d) show the SOC differences for 4, 13, 21, and 53 weeks after launch, respectively. The solid red line represents the in-orbit reference SOC estimated by UKF using the battery current and voltage collected in-orbit as inputs. The dashed blue line represents the estimated SOC by the proposed technique. The dotted green line represents the battery SOC predicted through power budget analysis, and the dotted and dashed magenta line represents the battery SOC predicted through the SARIMA model.

In the power budget-based SOC, estimation error occurs due to the uncertainty of the power generation and consumption conditions, and the maximum error compared to the in-orbit reference SOC is the largest. In general, the power budget analysis predicts conservatively to minimize the possibility of battery fault cases. As a result, the power budget-based SOC in Fig. 18(a), (b), (c), and (d) produces the maximum depth of discharge (DOD) (23% to 28%) in all figures in Fig. 18.

The SOC estimation using the SARIMA model shows that it is impossible to reproduce the fluctuations due to non-periodic attitude changes and mission. In addition, the SOC estimation using SARIMA power prediction shows that the average error and the maximum error are decreased compared to the power budget analysis, but the values of the maximum DOD show a tendency of smaller than that of the in-orbit reference SOC. Therefore, when SARIMA-based power prediction is used for maximum mission design, it is possible to optimistically predict the battery SOC and consume its power beyond the normal range.

In the proposed SOC estimation technique, when the SOC is estimated with insufficient training data, the maximum error increase about 9%. However, as shown in Fig. 18, the SOC estimation error using the current and voltage predicted in the Bi-LSTM network decreases with the increasing training dataset. This decrease is due to the accuracy improvement of the battery current and voltage prediction models that produce inputs for the SOC estimation. And it is found that the estimated SOC is discharging in the eclipse and mission (i.e., image, attitude change, and downlink) duration and charging in the Sun duration.

Both the average error and the maximum error are essential for the development of satellite power simulator. And, the range of the maximum DOD value is critical for the maximum possible mission design. The proposed SOC estimation technique shows superior performance in average error, maximum error, and maximum DOD value than the conventional power budget and SARIMA power prediction.

The results of the maximum error on the first day of each month for the in-orbit reference SOC and the predicted SOC are shown in Fig. 19. The dashed blue line indicates the

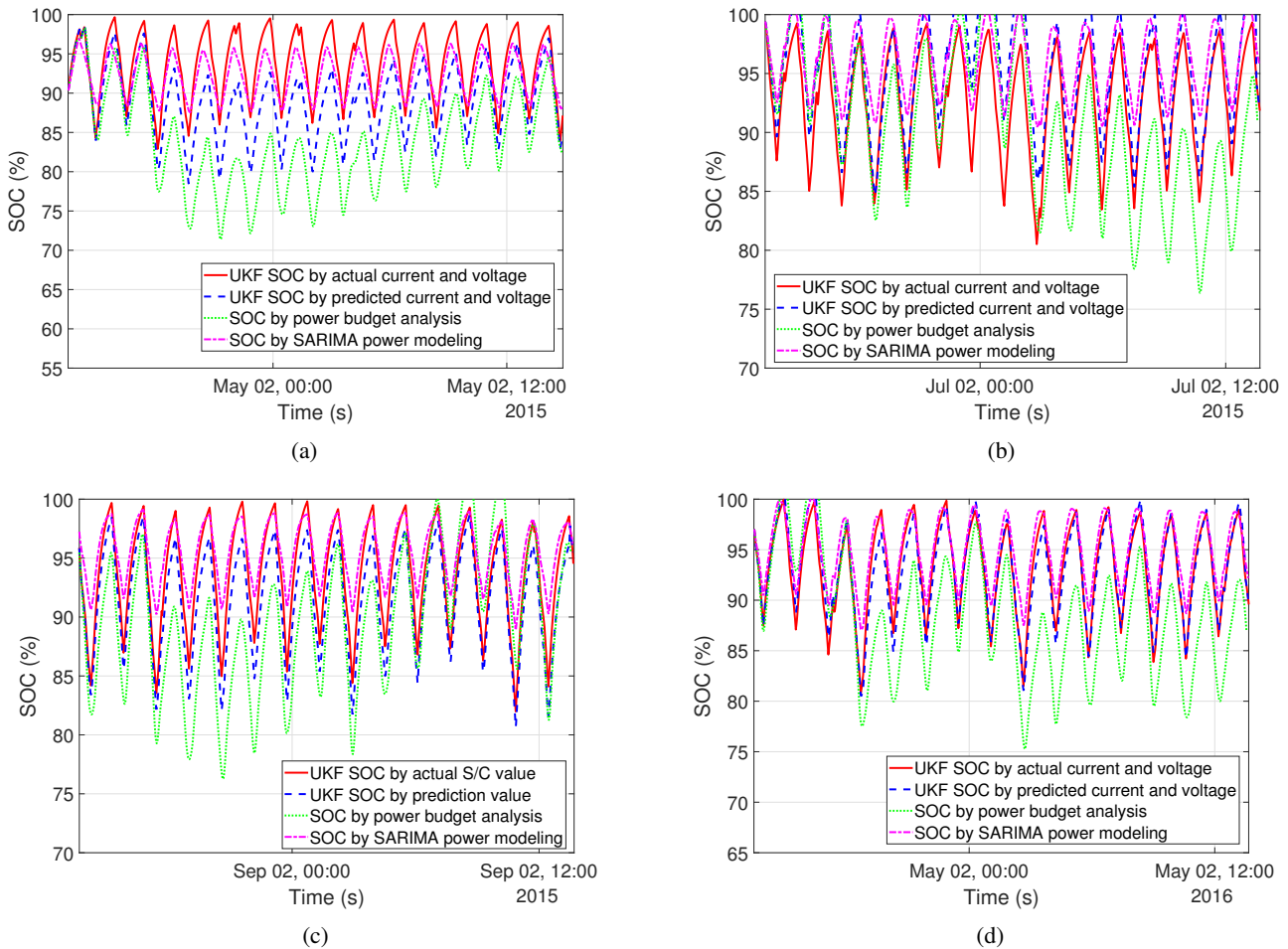


Fig. 18: SOC prediction results; (a) Result for May.2nd.2015; (b) Result for July.2nd.2015; (c) Result for September.2nd.2015; (d) Result for May.2nd.2016.

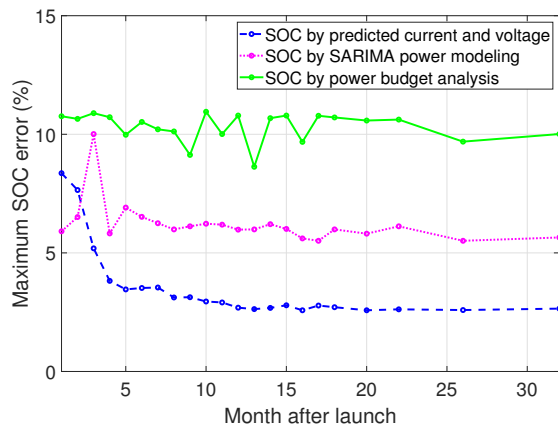


Fig. 19: Maximum SOC error of each prediction technique.

maximum error between in-orbit reference SOC and the SOC estimation using the current and voltage prediction data by the Bi-LSTM network, the dotted magenta line indicates the result of the SARIMA power model, and the solid green line indicates the result of the power budget analysis. For the max-

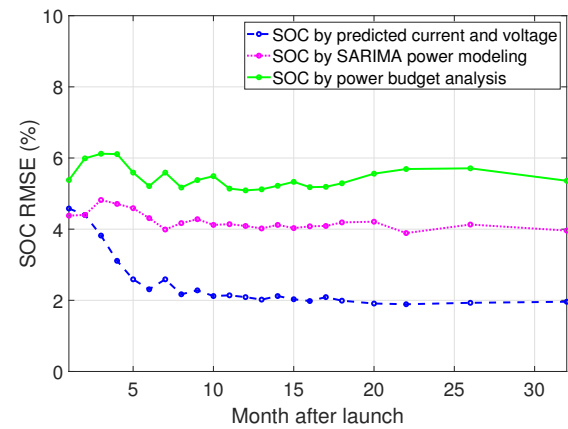


Fig. 20: SOC RMSE of each prediction technique.

imum error, the SOC estimation based on the power budget is consistently around 10% due to uncertainty factors. SOC prediction based on the SARIMA power model produces less maximum error than the proposed SOC estimation technique in the early stage when there is insufficient training data.

However, it is difficult to actively estimate changes in mission, trajectory, attitude, etc., so the maximum error is constantly around 6% for the SARIMA power model. However, in the proposed SOC estimation technique, the maximum error decreases as the data size used for training increases, and it is confirmed that it stabilizes within about 2.7%. It can be seen in the figure that the SOC estimation also becomes stabilized as the current and voltage errors decrease due to the update of the training dataset.

Figure 20 shows the RMSE between the in-orbit reference SOC and each SOC estimation result with respect to time after launch. The dashed blue line is for the proposed technique, the dotted magenta line indicates the SARIMA power modeling, and the solid green line shows the power budget analysis. SOC RMSE, by the power modeling based on power budget and SARIMA, maintains a specific level of error consistently. On the contrary, the RMSE of the proposed SOC estimation technique gradually decreases as the training dataset increases. Up to 12 months after launch, before the battery current and voltage prediction are stabilized, the SOC estimation RMSE of the proposed technique decreases from 4.28% to 2.05%. After the battery current and voltage prediction are stabilized, the RMSE of the proposed technique becomes as low as 2%.

## VI. CONCLUSION

In this paper, we have proposed a ground-based battery state estimation technique for LEO satellite systems using a UKF-based model that utilizes the battery current and voltage prediction by the Bi-LSTM network. To confirm the validity of the proposed technique, in-orbit current and voltage prediction errors are analyzed. And we have demonstrated the proposed ground-based battery state estimation technique by employing for the KOMPSAT-3A satellite. As a result, the proposed current and voltage prediction RMSE converge to about 1.7A and 0.2V, respectively. Furthermore, the proposed SOC estimation RMSE becomes about 2% compared to in-orbit reference SOC, including the non-contact duration, and the proposed technique has better performance than the conventional techniques. In conclusion, it is expected that applying the proposed technique to LEO satellites can facilitate the design of the maximum possible missions based on ground operation and provide guidance for satellite battery management protection.

Future research may predict battery current and voltage under normal and safe mode conditions and analyze battery fault detection.

## REFERENCES

- [1] Christopher Hendricks, Nick Williard, Sony Mathew, Michael Pecht, "A failure modes, mechanisms, and effects analysis (FMMEA) of lithium-ion batteries," *Journal of Power Sources*, vol. 297, pp. 113–120, 2015.
- [2] Y. Nishi, "Lithium ion secondary batteries; past 10 years and the future," *Journal of Power Sources*, vol. 100, pp. 101–106, Nov. 2001.
- [3] B. Scrosati and J. Garche, "Lithium batteries: Status, prospects and future," *Journal of Power Sources*, vol. 195, no.9, pp. 2419-2430, May. 2010.
- [4] J. Zhang and J. Lee, "A review on prognostics and health monitoring of Li-ion battery," *Journal of Power Sources*, vol. 196, pp. 6007–6014, Aug. 2011.
- [5] N. M. Vichare and M. G. Pecht, "Prognostics and health management of electronics," in *IEEE Transactions on Components and Packaging Technologies*, vol. 29, no. 1, pp. 222-229, March 2006, doi: 10.1109/TCAPT.2006.870387.
- [6] A. Wadi, M. F. Abdel-Hafez, A. A. Hussein and F. Alkhawaja, "Alleviating Dynamic Model Uncertainty Effects for Improved Battery SOC Estimation of EVs in Highly Dynamic Environments," in *IEEE Transactions on Vehicular Technology*, vol. 70, no. 7, pp. 6554-6566, July 2021, doi: 10.1109/TVT.2021.3085006.
- [7] S. Chen, J. G. and X. Ma, "Satellite On-Orbit Anomaly Detection Method Based on a Dynamic Threshold and Causality Pruning," in *IEEE Access*, vol. 9, pp. 86751-86758, 2021, doi: 10.1109/ACCESS.2021.3088439.
- [8] M. Uno and K. Tanaka, "Spacecraft Electrical Power System using Lithium-Ion Capacitors," in *IEEE Transactions on Aerospace and Electronic Systems*, vol. 49, no. 1, pp. 175-188, Jan. 2013, doi: 10.1109/TAES.2013.6404097.
- [9] C. A. Hill, "Satellite battery technology — A tutorial and overview," in *IEEE Aerospace and Electronic Systems Magazine*, vol. 26, no. 6, pp. 38-43, June 2011, doi: 10.1109/MAES.2011.5936184.
- [10] Z. Miao, L. Xu, V. R. Disfani and L. Fan, "An SOC-Based Battery Management System for Microgrids," in *IEEE Transactions on Smart Grid*, vol. 5, no. 2, pp. 966-973, March 2014, doi: 10.1109/TSG.2013.2279638.
- [11] J. P. Roselyn, A. Ravi, D. Devaraj and R. Venkatesan, "Optimal SoC Estimation Considering Hysteresis Effect for Effective Battery Management in Shipboard Batteries," in *IEEE Journal of Emerging and Selected Topics in Power Electronics*, vol. 9, no. 5, pp. 5533-5541, Oct. 2021, doi: 10.1109/JESTPE.2020.3034362.
- [12] H. Aung, J. J. Soon, S. T. Goh, J. M. Lew and K. -S. Low, "Battery Management System With State-of-Charge and Opportunistic State-of-Health for a Miniaturized Satellite," in *IEEE Transactions on Aerospace and Electronic Systems*, vol. 56, no. 4, pp. 2978-2989, Aug. 2020, doi: 10.1109/TAES.2019.2958161.
- [13] M. A. Hannan et al., "SOC Estimation of Li-ion Batteries With Learning Rate-Optimized Deep Fully Convolutional Network," in *IEEE Transactions on Power Electronics*, vol. 36, no. 7, pp. 7349-7353, July 2021, doi: 10.1109/TPEL.2020.3041876.
- [14] X. Shu, G. Li, Y. Zhang, S. Shen, Z. Chen and Y. Liu, "Stage of Charge Estimation of Lithium-Ion Battery Packs Based on Improved Cubature Kalman Filter With Long Short-Term Memory Model," in *IEEE Transactions on Transportation Electrification*, vol. 7, no. 3, pp. 1271-1284, Sept. 2021, doi: 10.1109/TTE.2020.3041757.
- [15] Y. Liu et al., "A Nonlinear Observer SOC Estimation Method Based on Electrochemical Model for Lithium-Ion Battery," in *IEEE Transactions on Industry Applications*, vol. 57, no. 1, pp. 1094-1104, Jan.-Feb. 2021, doi: 10.1109/TIA.2020.3040140.
- [16] S. Wang, C. Fernandez, L. Shang, Z. Li, and J. Li, "Online state of charge estimation for the aerial lithium-ion battery packs based on the improved extended Kalman filter method," *Journal of Energy Storage*, vol. 9, pp. 69-83, 2 Feb. 2017, doi: <http://dx.doi.org/10.1016/j.est.2016.09.008>.
- [17] H. Aung and K. S. Low, "Temperature dependent state-of-charge estimation of lithium ion battery using dual spherical unscented Kalman filter," *IET Power Electron.*, vol. 8, no. 10, pp. 2026-2033, Oct. 2015, doi: 10.1049/iet-pel.2014.0863.
- [18] Y. Zhou, M. Dong and J. Wu, "Hyperparameter Optimization for SOC Estimation by LSTM with Internal Resistance," *2021 International Conference on Computer Network, Electronic and Automation (ICCNEA)*, 2021, pp. 263-267, doi: 10.1109/ICCNEA53019.2021.00065.
- [19] X. Chen, W. Shen, M. Dai, Z. Cao, J. Jin and A. Kapoor, "Robust Adaptive Sliding-Mode Observer Using RBF Neural Network for Lithium-Ion Battery State of Charge Estimation in Electric Vehicles," in *IEEE Transactions on Vehicular Technology*, vol. 65, no. 4, pp. 1936-1947, April 2016, doi: 10.1109/TVT.2015.2427659.
- [20] D. N. T. How, M. A. Hannan, M. S. H. Lipu, K. S. M. Sahari, P. J. Ker and K. M. Muttaqi, "State-of-Charge Estimation of Li-Ion Battery in Electric Vehicles: A Deep Neural Network Approach," in *IEEE Transactions on Industry Applications*, vol. 56, no. 5, pp. 5565-5574, Sept.-Oct. 2020, doi: 10.1109/TIA.2020.3004294.
- [21] J. Meng, G. Luo and F. Gao, "Lithium Polymer Battery State-of-Charge Estimation Based on Adaptive Unscented Kalman Filter and Support Vector Machine," in *IEEE Transactions on Power Electronics*, vol. 31, no. 3, pp. 2226-2238, March 2016, doi: 10.1109/TPEL.2015.2439578.
- [22] F. A. Gers and E. Schmidhuber, "LSTM recurrent networks learn simple context-free and context-sensitive languages," in *IEEE Transactions on Neural Networks*, vol. 12, no. 6, pp. 1333-1340, Nov. 2001, doi: 10.1109/72.963769.
- [23] M. Ma and Z. Mao, "Deep-Convolution-Based LSTM Network for Remaining Useful Life Prediction," in *IEEE Transactions on Indus-*

- trial Informatics, vol. 17, no. 3, pp. 1658-1667, March 2021, doi: 10.1109/TII.2020.2991796.
- [24] K. Greff, R. K. Srivastava, J. Koutník, B. R. Steunebrink and J. Schmidhuber, "LSTM: A Search Space Odyssey," in IEEE Transactions on Neural Networks and Learning Systems, vol. 28, no. 10, pp. 2222-2232, Oct. 2017, doi: 10.1109/TNNLS.2016.2582924.
- [25] S. K. Ibrahim, A. Ahmed, M. A. E. Zeidan and I. E. Ziedan, "Machine Learning Methods for Spacecraft Telemetry Mining," in IEEE Transactions on Aerospace and Electronic Systems, vol. 55, no. 4, pp. 1816-1827, Aug. 2019, doi: 10.1109/TAES.2018.2876586.
- [26] X. Hu and Q. Yuan, "Epileptic EEG Identification Based on Deep Bi-LSTM Network," 2019 IEEE 11th International Conference on Advanced Infocomm Technology (ICAIT), 2019, pp. 63-66, doi: 10.1109/ICAIT.2019.8935899.
- [27] T. Dai, L. Zhu, Y. Wang and K. M. Carley, "Attentive Stacked Denoising Autoencoder With Bi-LSTM for Personalized Context-Aware Citation Recommendation," in IEEE/ACM Transactions on Audio, Speech, and Language Processing, vol. 28, pp. 553-568, 2020, doi: 10.1109/TASLP.2019.2949925.
- [28] C. Hou, H. Han, Z. Liu and M. Su, "A Wind Direction Forecasting Method Based on Z Score Normalization and Long Short Term Memory," 2019 IEEE 3rd International Conference on Green Energy and Applications (ICGEA), 2019, pp. 172-176, doi: 10.1109/ICGEA.2019.8880774.
- [29] K. -R. Kim, Y. Kim and S. Park, "A Probabilistic Machine Learning Approach to Scheduling Parallel Loops With Bayesian Optimization," in IEEE Transactions on Parallel and Distributed Systems, vol. 32, no. 7, pp. 1815-1827, 1 July 2021, doi: 10.1109/TPDS.2020.3046461.
- [30] H. Cho, Y. Kim, E. Lee, D. Choi, Y. Lee and W. Rhee, "Basic Enhancement Strategies When Using Bayesian Optimization for Hyperparameter Tuning of Deep Neural Networks," in IEEE Access, vol. 8, pp. 52588-52608, 2020, doi: 10.1109/ACCESS.2020.2981072.
- [31] I. Jokić, Ž. Žečević and B. Krstajić, "State-of-charge estimation of lithium-ion batteries using extended Kalman filter and unscented Kalman filter," 2018 23rd International Scientific-Professional Conference on Information Technology (IT), 2018, pp. 1-4, doi: 10.1109/SPIT.2018.8350462.
- [32] J. Meng, G. Luo and F. Gao, "Lithium Polymer Battery State-of-Charge Estimation Based on Adaptive Unscented Kalman Filter and Support Vector Machine," in IEEE Transactions on Power Electronics, vol. 31, no. 3, pp. 2226-2238, March 2016, doi: 10.1109/TPEL.2015.2439578.
- [33] Jaemoon Lee, Oanyong Nam, and B.H. Cho, "Li-ion battery SOC estimation method based on the reduced order extended Kalman filtering," Journal of Power Sources, vol. 174, no.1, pp. 9-15, Nov. 2007.
- [34] Seongjun Lee, Jonghoon Kim, Jaemoon Lee, and B.H. Cho, "State-of-charge and capacity estimation of lithium-ion battery using a new open-circuit voltage versus state-of-charge," Journal of Power Sources, vol.185, no. 2, pp. 1367-1373, Dec. 2008.
- [35] J. Kim, J. Shin, C. Jeon and B. Cho, "High accuracy state-of-charge estimation of Li-Ion battery pack based on screening process," 2011 Twenty-Sixth Annual IEEE Applied Power Electronics Conference and Exposition (APEC), 2011, pp. 1984-1991, doi: 10.1109/APEC.2011.5744869.
- [36] L. Ren, L. Zhao, S. Hong, S. Zhao, H. Wang and L. Zhang, "Remaining Useful Life Prediction for Lithium-Ion Battery: A Deep Learning Approach," in IEEE Access, vol. 6, pp. 50587-50598, 2018, doi: 10.1109/ACCESS.2018.2858856.
- [37] D. Haifeng, W. Xuezhe and S. Zechang, "A new SOH prediction concept for the power lithium-ion battery used on HEVs," 2009 IEEE Vehicle Power and Propulsion Conference, 2009, pp. 1649-1653, doi: 10.1109/VPPC.2009.5289654.
- [38] P. Chen, T. Pedersen, B. Bak-Jensen and Z. Chen, "ARIMA-Based Time Series Model of Stochastic Wind Power Generation," in IEEE Transactions on Power Systems, vol. 25, no. 2, pp. 667-676, May 2010, doi: 10.1109/TPWRS.2009.2033277.
- [39] V. Kushwaha and N. M. Pindoriya, "Very short-term solar PV generation forecast using SARIMA model: A case study," 2017 7th International Conference on Power Systems (ICPS), 2017, pp. 430-435, doi: 10.1109/ICPES.2017.8387332.



management operation.

**Seok-Teak Yun** received his B.S. degree in electrical engineering from Postech, Pohang, Korea in 2005, his M.S. degree in electrical engineering and computer science from the Seoul National University, Seoul, Korea in 2007, and received Ph.D. in robotics at Korea Advanced Institute of Science and Technology (KAIST), Deajeon, Korea in 2022. He joined the Korea Aerospace Research Institute (KARI) in 2007. He is a Senior Researcher in KARI and main research interests include batteries, power control systems, satellite mission design, and fault



**Seung-Hyun Kong** (M'06–SM'16) is an Associate Professor in the CCS Graduate School of Green Transportation of Korea Advanced Institute of Science and Technology (KAIST), where he has been a faculty member since 2010. He received a B.S. degree in Electronics Engineering from Sogang University, Seoul, Korea, in 1992, an M.S. degree in Electrical and Computer Engineering from Polytechnic University (merged to NYU), New York, in 1994, a Ph.D. degree in Aeronautics and Astronautics from Stanford University, Palo Alto, in 2005. From 1997 to 2004 and from 2006 to 2010, he was with companies including Samsung Electronics (Telecommunication Research Center), Korea, and Qualcomm (Corporate R&D Department), San Diego, USA for advanced technology R&D in mobile communication systems, wireless positioning, and assisted GNSS. Since he joined KAIST as a faculty member in 2010, he has been working on various R&D projects in advanced intelligent transportation systems, such as robust GNSS-based navigation for urban environment, deep learning and reinforcement learning algorithms for autonomous vehicles, sensor fusion, and vehicular communication systems (V2X). He has authored more than 100 papers in peer-reviewed journals and conference proceedings and 12 patents, and his research group won the President Award (of Korea) in the 2018 international student autonomous driving competition host by the Korean government. He has served as an associate editor of IEEE T-ITS and IEEE Access, an editor of IET-RSN and the lead guest editor of the IEEE T-ITS special issue on "ITS empowered by AI technologie" and the IEEE Access special section on "GNSS, Localization, and Navigation Technologies". He has served as the program chair of IPNT from 2017 to 2019 in Korea and as a program co-chair of IEEE ITSC2019, New Zealand.